Icosahedron Oligomerization and Condensation in Intermetallic Compounds. Bonding and Electronic Requirements

Monique Tillard-Charbonnel,* Alain Manteghetti, and Claude Belin

Laboratoire des Agrégats Moléculaires et Matériaux Inorganiques, CC015, Université Montpellier II, Sciences et Techniques du Languedoc, 2 Place Eugène Bataillon, 34095 Montpellier Cedex 5, France

Received September 9, 1999

Icosahedron-based clustering has been found to be very common in intermetallics, particularly for group 13 and early p-block icosogen elements. Linking of the icosahedral building blocks depends on the valence electron concentrations. Vertex-, edge-, or face-sharing icosahedra occur as the structure compensates for electron deficiency. Some examples of icosahedron-based clusters have been selected for an analysis of the relationships between the structural features (icosahedron oligomerization, atomic defects, etc.) and the bonding and electronic requirements. The extended Hückel method has been used with either a molecular approach or an electronic band structure calculation to rationalize bonding in the intermetallic framework.

Icosahedral packing very often occurs in intermetallic compounds in which the elements have metallic radii in a ratio close to $5^{1/4}\tau^{1/2} - 1$ (0.902), where τ is the golden number. Elements which have a greater tendency to coordinate icosahedrally are Mn, Fe, Mo, W, Cu, Zn, and Cd. The group 13 elements B, Al, Ga, In, and Tl can also form icosahedral, and most often empty, clusters; such elements have been given the name "icosogen".[1] Even some elements of group 14, such as Si or Sn, are able, under certain conditions, to display similar behavior.

In compounds containing alkali (or alkaline-earth) metals and group 12 or 13 elements, the electronegative but electron-poor elements are reduced by the electropositive elements. In accordance with the Zintl−Klemm formalism, these compounds form anionic frameworks that are generally built of icosahedral clusters.

For a cluster, the polyhedral electron count (PEC) is defined as the total number of electrons required for stabilization. Subtracting from the PEC the number of electrons involved in exo (cluster-to-ligand or intercluster) bonding or in nonbonding pairs leads to the number of electrons available for skeletal bonds. Usually, skeletal bonding is quantified by the number of skeletal electron pairs (SEP), which is one-half of the skeletal electron count (SEC). The valence electron count (VEC) is equal to the SEC plus the number of nonbonding electrons plus one-half of the number of exo-bond electrons.

The linking of icosahedral units within structures is very dependent upon the number of valence electrons. In the most reduced phases, VECs may be high and equal to the Wade−Mingos polyhedral electron requisite for naked clusters, defined as the PEC; in these conditions, the icosahedra are not linked to adjacent units. In less reduced phases, such as those having a small content of the electropositive element, the VEC is lower than the PEC, and linking between icosahedra is required to minimize this electron deficiency through the sharing of electrons. In cases of severe electron deficiencies, icosahedra may condense through vertex, edge, or face sharing to form oligomeric moieties.

This paper will present and analyze, with selected examples chosen among icosahedron-containing compounds, the bonding and optimal electronic requirements for the linking and condensation of icosahedral clusters within different classes of intermetallic compounds. In the following, we will report results obtained from extended Hückel calculations. In accord with Zintl−Klemm theory, alkali metal atoms were considered to be one-electron donors and were not taken into account in the calculations.

Discrete Icosahedral Clusters

Understanding of the chemical bonds within icosahedral clusters was promoted in the early 1950s by crystallographic studies and semiempirical molecular orbital calculations. Using the MO−LCAO method, Longuet-Higgins analyzed the stability of a regular boron icosahedron and also predicted the existence of the $B_{12}H_{12}^{2-}$ boron hydride.[2] Bonding therein can not be described in terms of localized covalent bonds in the sense that there are not enough electrons to form classical two-center, two-electron (2c-2e) bonds along each edge of the polyhedron. Results of MO calculations indicate that the icosahedron skeleton is stabilized with 26 (skeletal) electrons, while 24 ("exo") electrons are involved in B−H exo bonding, so the PEC is 50 for the icosahedron.

These findings feature the polyhedral skeletal electron pair theory (PSEPT) that was developed later by Wade,[3] Mingos,[4,5] Williams,[6] and Rudolph.[7] These basic rules are now referred to as Wade's rules. A closed deltahedral (*closo*) cluster skeleton with n vertexes is stabilized with $n + 1$ bonding SEPs. The geometry-related *nido*, *arachno*, and *hypho* cluster skeletons, with respectively $n - 1$, $n - 2$, and $n - 3$ vertexes, are also

* E-mail: mtillard@univ-montp2.fr.

(1) King, R. B. *Inorg. Chem.* **1989**, *28*, 2796.
(2) Longuet-Higgins, H. C.; de V. Roberts, M. *Proc. R. Soc.* **1954**, *A224*, 336; **1955**, *A230*, 110.
(3) Wade, K. *J. Chem. Soc., Chem. Commun.* **1971**, 792; *Adv. Inorg. Chem. Radiochem.* **1976**, *18*, 1.
(4) Mingos, D. M. P. *Nature, Phys. Sci.* **1972**, *236*, 99.
(5) Mingos, D. M. P.; Wales, D. J. *Introduction to Cluster Chemistry*; Prentice Hall: Englewood Cliffs, NJ, 1990.
(6) Williams, R. E. *Inorg. Chem.* **1971**, *10*, 210.
(7) Rudolph, R. W. *Acc. Chem. Res.* **1976**, *9*, 446.

10.1021/ic9910817 CCC: $19.00
Published on Web 03/29/2000

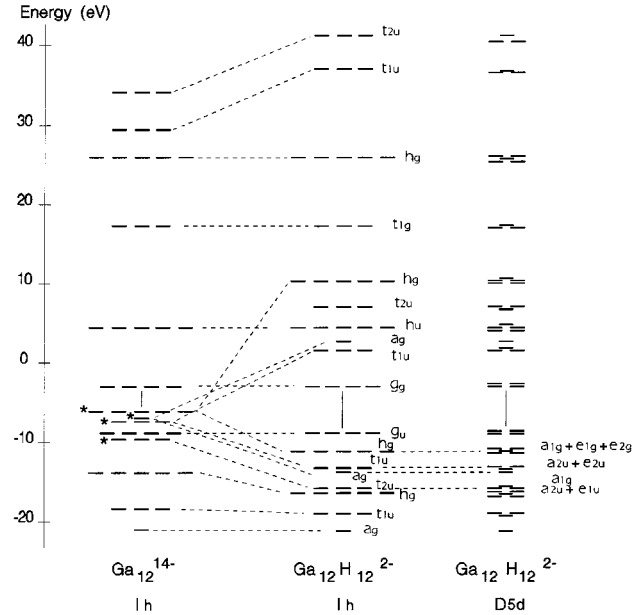

Figure 1. Energy diagrams (from EHMO calculations) for discrete icosahedral units: left, Ga_{12}^{14-} (I_h symmetry, asterisks mark levels having exo character); middle, $Ga_{12}H_{12}^{2-}$ (I_h symmetry); and right, $Ga_{12}H_{12}^{2-}$ (D_{5d} symmetry). Saturation with hydrogen ligands stabilizes the 12 radial (exo) orbitals a_g, t_{1u}, t_{2u}, and h_g. Along the I_h to D_{5d} distortion, these levels are split into a_{1g}, $a_{2u} + e_{2u}$, $a_{2u} + e_{1u}$, and $a_{1g} + e_{1g} + e_{2g}$, respectively.

stabilized with $n + 1$ skeletal electron pairs. These cluster skeletons are increasingly electron-rich and lose deltahedral faces to form open polyhedra with more localized bonding. These rules have been supplemented with capping and condensation principles that provide some rationalization for the complex structures built from simple polyhedral units.[8] The skeletal electron count for a condensed cluster is equal to the sum of skeletal counts of the parent clusters minus the count for the shared unit (atom, edge, or face).

Isolated icosahedral clusters, not connected to neighboring units, would have high anionic charges (-14 for an empty icosahedron, such as Ga_{12}^{14-}) with respect to the closed-shell requirement (PEC = 50). Some examples of discrete Tl-centered thallium icosahedra have been found in the intermetallic systems of thallium and alkali metals,[9,10] making these clusters highly "solvated" and somewhat polarized by the alkali countercations.

However, in extended structures, icosahedral clusters can reduce their anionic charge by connecting to surrounding units (atoms or clusters), generally through 2c-2e bonds. Now, with 12 exo bonds similar to the B−H bonds in $B_{12}H_{12}^{2-}$, the icosahedra have a lower anionic charge (-2). Energy-level diagrams for M_{12}^{14-} and $M_{12}H_{12}^{2-}$ are represented in Figure 1 for gallium units. These anionic species have the same electron count (25 filled molecular orbitals stabilized in the bonding domain). Saturation of the naked cluster with hydrogen ligands has a stabilizing effect: the gap is increased, and the highly degenerate h_g orbital, which is the HOMO for the naked cluster, drops in energy below the g_u orbital, the HOMO for the H-saturated cluster. A slight elongation of the icosahedral unit along the 5-fold axis ($I_h \rightarrow D_{5d}$) lowers the level of degeneracy (see Figure 1) but does not change the energy diagram or the electron count. Elongation along the 3-fold or 2-fold axis ($I_h \rightarrow D_{3d}$ or $I_h \rightarrow C_{2v}$, respectively) would have similar effects.

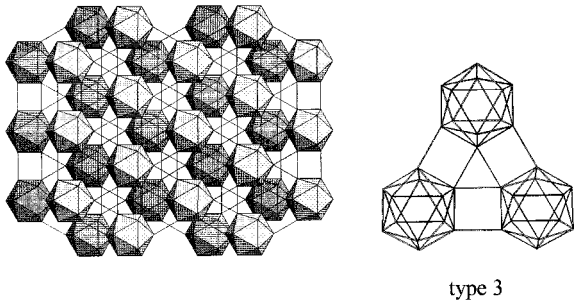

Figure 2. Representation of the polyhedral packing along $\vec{c}$ in rhombohedral $RbGa_7$ (left) and the particular bonding (type 3) involving 3c-2e bonds (right).

Scheme 1

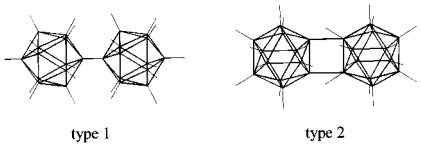

Linked Individualized Icosahedra

In molecular species as well as in extended structures, icosahedral units suffer some atomic defects; numerous examples are known in boron chemistry and in gallium intermetallics. For the *nido* icosahedron $M_{11}H_{11}^{2-}$ (PEC = 48), the skeletal electron count of 26 is still retained, whereas only 22 electrons are involved in exo bonding. In *arachno* $M_{10}H_{10}^{2-}$, Wade's rules fail when two or three adjacent atoms are removed (iso-*arachno*); the skeletal electron count is then reduced to 22 or 20, respectively.[11] Although 5-fold symmetry is not allowed in periodic frameworks, extended icosahedral structures may exist with some lattice distortions. In YB_{66}, for example, the B_{12} icosahedral unit is linked to 12 icosahedra, but the 5-fold symmetry is restricted to one shell around the icosahedron and, beyond this shell, is broken by the presence of low-coordinate and disordered boron atoms.

The most simple way for two icosahedra to be connected is by direct bonding between two apexes; this is commonly observed in M_xGa_y phases (M = alkali metal).[12] For the two models depicted in Scheme 1, intericosahedral bonds are 2c-2e classical bonds, and the PECs are 98 and 96, respectively.

Noteworthy is the linking observed in $RbGa_7$,[13,14] in which the icosahedron is connected, in its medial plane, to six adjacent icosahedra (Figure 2) by 3c-2e bonds (bonding type 3). The coordination of the icosahedron to six other icosahedra, three above and three below, is achieved with 2c-2e bonds. The PEC is still 50, but because of the presence of 3c-2e bonds, the VEC is $36 = 26 + (6 \times 2)/3 + (6 \times 2)/2$ [instead of $38 = 26 + (12 \times 2)/2$ for an icosahedron with 12 2c-2e exo bonds]. This bonding scheme represents a primary step toward condensation of icosahedra.

Extended Structures Containing Separated Icosahedra

In this section, we will describe extended structures in which icosahedra are no longer linked to each other by classical 2c-2e bonds or (as analyzed later) by vertex, edge, or face sharing.

(8) Mingos, D. M. P. *Acc. Chem. Res.* **1984**, *17*, 311.
(9) Blase, W.; Cordier, G.; Somer, M. *Z. Kristallogr.* **1991**, *194*, 150.
(10) Corbett, J. D. In *Chemistry, Structure and Bonding in Zintl Phases and Ions*; Kauzlarich, S., Ed.; VCH.: New York, 1996.
(11) Burdett, J. K.; Canadell, E. *J. Am. Chem. Soc.* **1990**, *112*, 7207.
(12) Belin, C.; Tillard, M. *Prog. Solid State Chem.* **1993**, *22* (2), 59.
(13) Belin, C. *Acta Crystallogr.* **1981**, *B37*, 2060.
(14) Belin, C.; Tillard-Charbonnel, M. *Coord. Chem. Rev.* **1998**, *178*, 529.

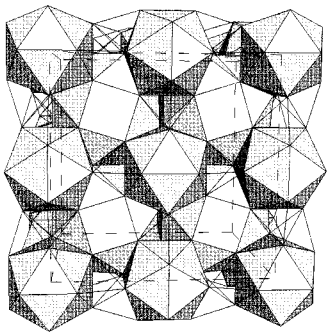

Figure 3. Representation of the $NaZn_{13}$ cubic cell.

Scheme 2

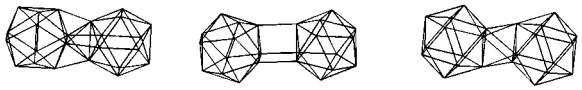

In the examples illustrated in Scheme 2, icosahedra are connected through a shared tetrahedron (type 4), a shared trigonal prism (type 5), and a shared trigonal antiprism (type 6) with delocalized bonding. It appears that, in the case of regular icosahedra, connection through a shared tetrahedron also implies the sharing of four adjoining tetrahedra.

We will focus on two models of bonding, type 4 and type 6, found in the $NaZn_{13}$ and $MoAl_{12}$ structures, respectively. In both cases, there is a centering atom inside the icosahedron. Then, a comparison with the Zintl compound $K_6(NaCd)_2Tl_{12}Cd$ will be proposed.

$NaZn_{13}$. $NaZn_{13}$ crystallizes in the cubic system (*Fm*3*c*, a = 12.283 Å)[15] and is isostructural with KZn_{13} and KCd_{13}. Zinc atoms form a Zn-centered icosahedron at the (0, 0, 0) position. The *fcc* Bravais cell contains eight icosahedra (Figure 3). Each of these icosahedra is linked along the ⟨100⟩ direction to six adjacent icosahedra through shared tetrahedra (type 4 bonding) that are built with two cross edges of adjoining icosahedra.

Twelve faces of the icosahedron, two on each side of the ⟨100⟩ edges, form tetrahedra with the apexes of the adjoining icosahedra. Noteworthy are the intericosahedral bonds (2.572 and 2.682 Å) that are shorter than intraicosahedral bonds (2.764 and 2.929 Å). Sodium atoms ($^1/_4$, $^1/_4$, $^1/_4$) occupy intericosahedral voids inside a 24-Zn snub cube comprising 32 triangular and 6 square faces.

To analyze the bonding between two adjacent icosahedral units, we first performed an extended Hückel calculation (EHMO) for a $(Zn_{12}H_8)_2$ molecular unit (Scheme 2, type 4) in which apexes not involved in interpolyhedral bonds were saturated with hydrogen atoms. Such a unit requires 92 electrons, of which 60 are skeletal electrons, to reach a closed-shell configuration. As previously observed,[16] the centering of the icosahedra by Zn atoms does not change the polyhedral electron count. Because the skeletal electron count for a single icosahedron is 26, the linked icosahedral units would have 60 − (2 × 26) = 8 electrons for intericosahedral bonding, that is, four 4c-2e bonds. Because each icosahedron has six interconnections, its VEC, according to this analysis, would be 26 + $^8/_2$ × 6 = 50, which is quite unlikely because that value is as large as the PEC for an isolated icosahedron!

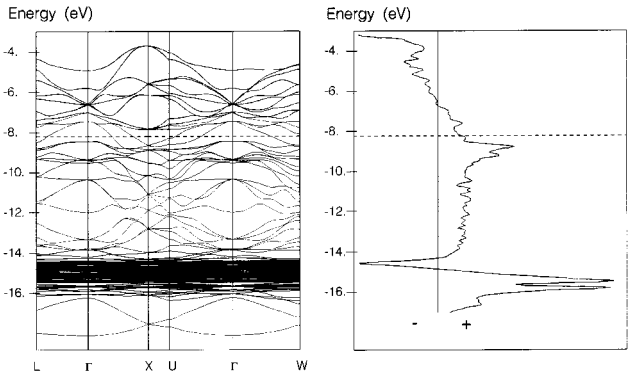

Figure 4. Band structure for $NaZn_{13}$ (left). Crystal orbital overlap population (COOP) curves for all Zn−Zn interactions in $NaZn_{13}$ (right). The dotted line at −8.1 eV indicates the Fermi level for 314 electrons.

A more detailed understanding of the bonding and electronic structure of the linked icosahedral units can be achieved by a three-dimensional band calculation[17] and a density-of-states (DOS) analysis.[18]

We used an effective Hamiltonian of the extended Hückel type.[19] Band structure (Figure 4) was calculated for 25 k-points along special symmetry paths in the Brillouin zone of the primitive cell (two icosahedral units), and densities of states were calculated for a set of 56 k-points in the irreducible Brillouin zone (IBZ).

It appears that a group of bands that are almost exclusively Zn 3d in character stays at an energy level close to the Zn 3d orbital energy. This fact indicates that a large fraction of these orbitals do not play an important role in the electronic structure of the cluster. Contributions from atomic orbitals of the two types of Zn atoms to the total DOS indicate that the 3d levels of the zinc atoms at the surface of the icosahedron are slightly involved in bonding whereas those of the centering zinc atom are not involved at all. Crystal orbital overlap population (COOP) curves[20] show that the optimal situation in terms of bonding (closed shell) would be reached for an electron population of 324, leading to a count of 162 electrons per formula unit. This is in good agreement with the results (LMTO and ELF) recently published for a series of $NaZn_{13}$-type ternary compounds.[21] The actual Fermi level for $NaZn_{13}$ (314 electrons, including Zn 3d electrons) crosses a low density-of-states continuum that provides this material with a poor metallic character.

$MoAl_{12}$. $MoAl_{12}$, isotypic with MAl_{12} (M = Mn or Cr), crystallizes in the $Im\bar{3}$ cubic space group with a = 7.576 Å.[22] (See Figure 5.) The unit cell contains two Mo-centered aluminum icosahedra (one per primitive rhombohedral cell). The structure packing along ⟨100⟩ is different from that in $NaZn_{13}$, because the icosahedra are aligned by facing parallel edges. Each icosahedron is linked to 6 alike units through 12 direct bonds (2.893 Å) and to 8 others along ⟨111⟩ by sharing pseudo-octahedra (intericosahedral bonds of 2.797 Å).

Bonding between two icosahedra sharing an antiprism (pseudo-octahedron) can be analyzed by EHMO, first in the approximation of a molecular dimer, $(Al_{12}H_8)_2$, (Scheme 2, type 6) in which 16 atoms that are not involved in intericosahedral bonding have been saturated with hydrogen atoms. Electronic

(15) Shoemaker, D. P.; Marsh, R. E.; Ewing, F. J.; Pauling, L. *Acta Crystallogr.* **1952**, *5*, 637.
(16) Tillard-Charbonnel, M.; Belin, C.; Manteghetti, A.; Flot, D. *Inorg. Chem.* **1996**, *35*, 2583.
(17) Whangbo, M. H.; Hoffmann, R. *J. Am. Chem. Soc.* **1978**, *100*, 6093.
(18) Hoffmann, R. *Angew. Chem., Int. Ed. Engl.* **1987**, *26*, 846.
(19) Hoffmann, R. *J. Chem. Phys.* **1963**, *39*, 1397.
(20) Hughbanks, T.; Hoffmann, R. *J. Am. Chem. Soc.* **1983**, *105*, 1150.
(21) Nordell, K. J.; Miller, G. J. *Inorg. Chem.* **1999**, *38*, 579.
(22) Adam, J.; Rich, J. B. *Acta Crystallogr.* **1954**, *7*, 813.

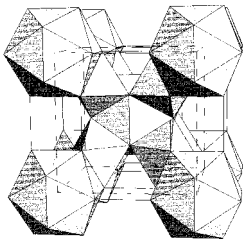

Figure 5. Polyhedral packing in the cubic cell of $MoAl_{12}$.

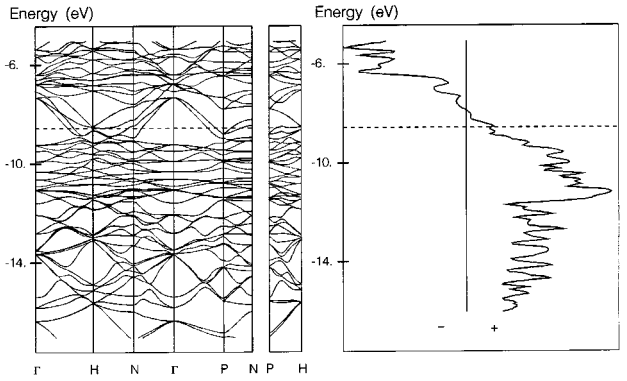

Figure 6. Band structure for $MoAl_{12}$ (left). COOP curves for all atom−atom interactions in $MoAl_{12}$ (right). The Fermi level is indicated at −8.52 eV for 42 electrons.

stabilization [closed shell, $(Al_{12}H_8)_2^{6-}$] of this unit requires 94 electrons, of which 36 are used for Al−H bonding and 58 for skeletal bonding. Icosahedron centering with a transition element does not change the overall Al−Al skeletal electron count but only the anionic charge. Subtracting from the total electron count of 94 the electrons for Al−H bonds (2×16) and the skeletal electron counts for the individual clusters (2×26) leaves 6 electrons for bonding within the shared pseudo-octahedron.

In the $MoAl_{12}$ three-dimensional framework, each icosahedron is doubly linked to six alike icosahedra. This linking involves parallel edges that approximately form a square (type 2). We consider, a priori, that these bonds (12 around each icosahedron) are 2c-2e. In addition, Al atoms are involved in octahedron sharing (type 6). Under these conditions, the valence electron count for one icosahedron should be $26 + 12 + 8 \times {}^6/_2 = 62$. This count is, of course, too large, which indicates that bonding in this phase is much more delocalized.

The three-dimensional band structure (25 k-points) indicates a large dispersion of bands (Figure 6) across the Fermi level (42 electrons for the primitive rhombohedral cell), in agreement with the metallic character of the compound. Because of their high energy, the Mo 4d orbitals are involved in bonding near the Fermi level. There are three crystal orbitals, which are degenerate at point Γ, that are cut by the Fermi level; they are primarily Mo $4d_{xy}$, $4d_{xz}$, and $4d_{yz}$ and Al 3p in character. Densities of states have been calculated for 112 k-points in the IBZ. Below the Fermi level, Al 3s and 3p orbitals are strongly mixed with the Mo 4d levels, whereas the Mo 5s and 5p orbitals make a very small contribution. Electron densities for Mo and Al atoms are close to 8.8 and 2.8, respectively, showing the electron-acceptor character of the centering transition metal atom, in accordance with the difference in electronegativity between the elements (1.8 and 1.5 for Mo and Al, respectively). Analysis of COOP curves (Figure 6) indicates that the system would reach a closed-shell configuration for 44 electrons. Additional electrons would destabilize the alloy by filling exclusively antibonding Mo−Al orbitals.

The compound $Na_4K_6Tl_{13}$,[23] $Im\bar{3}$, displays a stretched structure with respect to $MoAl_{12}$. Icosahedra of thallium are similarly packed, but sodium atoms are inserted at the 8(c) site ($\bar{3}$) at the center of the shared antiprism, and voids [12(e), mm] between the icosahedra are filled with potassium atoms. There is no longer direct linking between Tl-centered thallium icosahedra (one per unit cell), which have an open-shell PEC of 49, one electron short of the ideal count for an isolated icosahedron.

Linking through Interstitial Atoms. Bonding between two icosahedra along a 3-fold axis through the interaction of two adjoining triangular faces can be analyzed in the eclipsed D_{3h} or staggered D_{3d} configuration (Scheme 2, type 5 or 6, respectively). Schematically, intericosahedral bonding can be described satisfactorily with the use of six out-of-plane orbitals (radial sp type), three at each of the triangular faces. According to C_{3v} symmetry, the exo orbitals of each triangle provide a_1 and e fragment orbitals. The combination from the two triangular faces yields $a'_1 + a''_2 + e' + e''$ levels in case of the D_{3h} prismatic geometry and $a_{1g} + a_{2u} + e_g + e_u$ levels for the antiprismatic D_{3d} geometry (Figure 7). Incorporation of an interstitital atom inside the prism or the antiprism would have a stabilizing effect through the interactions of the exo orbitals of the triangles with the s and p AOs of the inserted atom. Between these models, there is no significant difference in the sum of one-electron energies; however, D_{3d} geometry is most often found in the solid state because it reduces steric constraints, thereby providing better crystal packing. Degenerate levels (e'' or e_g) are not involved in the case of main group interstitial elements, but they can interact with the d orbitals of a transition metal atom. Such interactions have been analyzed in the three-dimensional framework of the Zintl compound $K_6(NaCd)_2Tl_{12}Cd$.[16]

$K_6(NaCd)_2Tl_{12}Cd$. $K_6(Na_2Cd_2)Tl_{12}Cd$ crystallizes in the $Im\bar{3}$ cubic space group with $a = 11.321(2)$ Å.[16] The unit cell contains two Cd-centered thallium icosahedra that are packed in the same manner as in $MoAl_{12}$ and $Na_4K_6Tl_{13}$. However, in $K_6(NaCd)_2Tl_{12}Cd$, each icosahedron is coordinated by eight atoms, four Cd and four Na, at the apexes of a regular cube on the body diagonals of the unit cell. These atoms cap faces of two inverted icosahedra (Figure 8).

It has been shown that encapsulation of a Cd atom inside the Tl_{12} icosahedron does not greatly modify the MO energy diagram;[16] the centered $Tl_{12}Cd$ cluster has a PEC of 50. Interaction between $Tl_{12}Cd$ clusters through surrounding Cd atoms in the crystal can be qualitatively analyzed with the molecular interaction scheme (D_{3d} symmetry) depicted in Figure 7. Cd atomic orbitals combine with the MOs of the $(Tl_3)_2$ unit (two facing triangles) into four bonding MOs leaving two radial orbitals as nonbonding. This provides three filled levels (two bonding and one nonbonding) per Tl_3 unit, and because there are four outer Cd atoms around the $Tl_{12}Cd$ icosahedron, there are still 12 filled (8 bonding and 4 nonbonding) orbitals outside the icosahedral skeleton. Hence, the ideal count of 50 electrons is preserved.

Band structure calculations for the $K_6(NaCd)_2Tl_{12}Cd$ framework have been carried out in the full energy domain (Figure 9). Preliminary calculations indicated that Cd 4d orbitals had no important participation in the bonding, so they were not considered. Crystal orbital analysis at point Γ shows that the three almost-flat bands around −11.8 eV correspond to combinations of tangential Tl AOs on the surface of the icosahedron and remain free from any combination with Cd levels. A group

(23) Dong, Z. C.; Corbett, J. D. *J. Am. Chem. Soc.* **1995**, *117*, 6447.

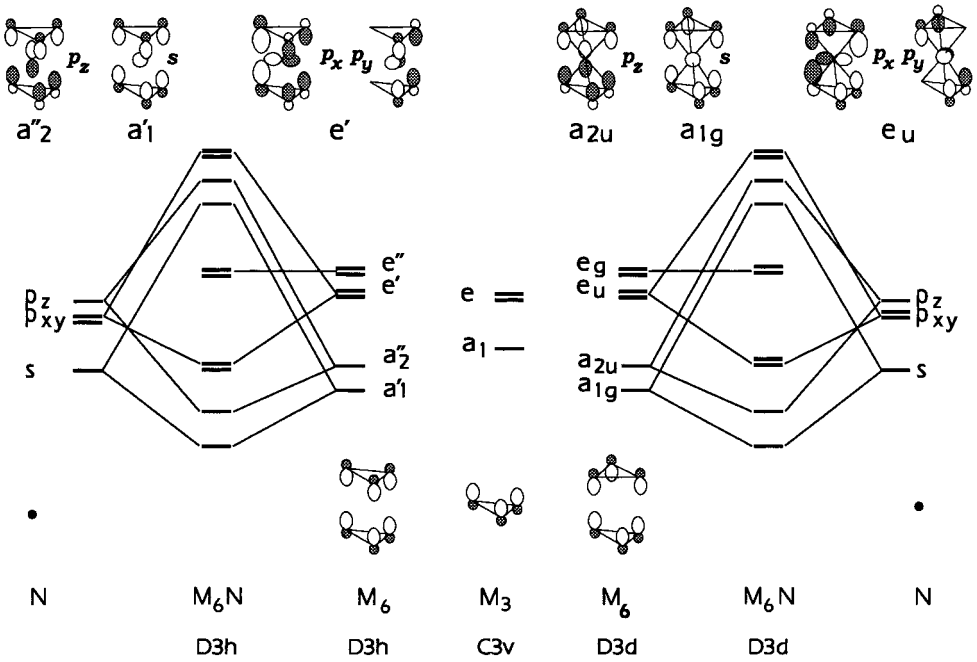

Figure 7. Schematic interaction diagram of intericosahedral bonding through an interstitial atom. Eclipsed D_{3h} (left) and staggered D_{3d} (right) configurations are considered.

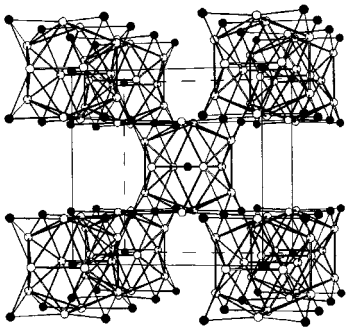

Figure 8. Representation of the atomic packing in the $K_6(NaCd)_2Tl_{12}Cd$ cubic cell. Solid circles represent Na and Cd atoms; for clarity, potassium atoms are omitted.

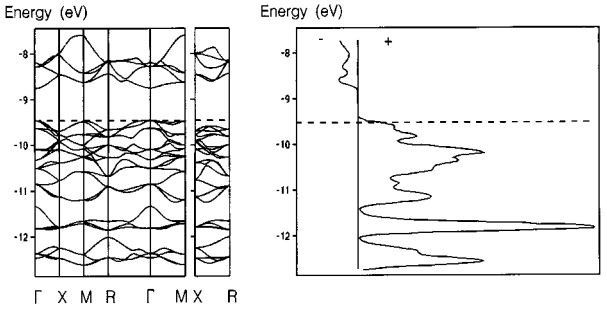

Figure 9. Band structure (left) and COOP curves (right) for an ordered model of $K_6(NaCd)_2Tl_{12}Cd$ (cubic cell with two independent icosahedral units). Fermi level is indicated for 100 electrons, that is, 50 electrons per icosahedral unit.

of three bands near −9.45 eV, just below the Fermi level, is not much dispersed. These bands essentially result from combinations of the Tl radial AOs and have no contribution from Cd atoms. They may be considered as unaltered nonbonding pairs of the molecular $Tl_{12}Cd$ unit. However, the outer Cd atoms (Cd_{out}) contribute in the domain between −9.8 and −11.2 eV, which makes the bands slightly more dispersed, with a total width of less than 0.6 eV, the bonding and antibonding domains being separated by a substantial gap of ∼0.6 eV. Noteworthy is the Tl−Cd_{out} bonding contribution just above −8.5 eV in the antibonding domain that results from overlap of the p_x and p_y orbitals of the outer Cd atom with the tangential skeletal orbitals (p in character) of the icosahedral units.

The strong Tl−Tl antibonding contribution is responsible for the destabilization of these levels. It has been shown that, up to the Fermi level, nearly half of the Cd_{out} states are filled, and bonding around the outer Cd atom can be schematically described with two 4c-2e bonds. This is supported by the Cd_{out} electron population of 1.9 calculated at the Fermi level. Populations of 1.7 and 3.7 have been found for the centering Cd (Cd_{int}) and for the Tl atoms, respectively. All of these findings suggest that molecular features of the $Tl_{12}Cd$ cluster are partially retained in the band structure, making the compound a semiconductor (in agreement with single-crystal electrical resistivity measurements).[16] The density of states (calculated with a set of 170 k-points) has a nearly zero value at the Fermi level (closed-shell compound). DOS contributions from the Tl and Cd_{out} atomic orbitals remain similar in shape throughout the energy domain, indicating the covalent nature of the interactions.

Condensed (or Fused) Icosahedra

Vertex-Sharing Icosahedra. This condensation mode is common for centered icosahedral clusters of late transition metals. Polycondensation (bi-icosahedra, tri-icosahedra, etc.) is well exemplified by the family of Au-rich clusters. As reported by Zhang and Teo,[24] the electronic requirements for such centered clusters are very specific. The radial bonding (centering Au-to-surface atoms) is stronger than the surface bonding, emphasizing the important role of the centering atom in the structure stabilization for this class of clusters. Here, the cluster terminology should be abandoned as these compounds are better described as coordination complexes.

Vertex-sharing icosahedra are also found in main-group element chemistry (boranes and carboranes) in which the shared atom is a transition metal.[25] For example, $Ni(C_2B_9H_{11})_2$ was described as a nickel(IV) ion sandwiched between two *nido*

(24) Zhang, H.; Teo, B. K. *Inorg. Chim. Acta* **1997**, *265*, 213.

Scheme 3

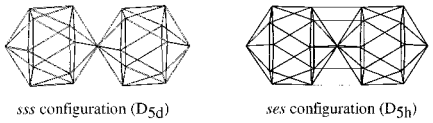

icosahedral fragments.[26] The two icosahedra are in the staggered-staggered-staggered (*sss*) configuration;[27] the molecule is centrosymmetric and displays the D_{5d} symmetry. Note that a staggered-eclipsed-staggered (*ses*) configuration of icosahedra would lead to a D_{5h} symmetry (see Scheme 3).

Two $C_2B_9H_{11}^{2-}$ *nido* icosahedra, each with an open pentagonal face such as the cyclopentadienyl ligand, are assumed to donate 6 electrons each to the transition metal atom to form these sandwich compounds. The most stable molecules, such as ferrocene, have an 18-electron central metal atom.

We have performed EHMO calculations for $Ni(C_2B_9H_{11})_2$ and for the hypothetic individual isohedron $NiC_2B_9H_{11}$. Condensed $Ni(C_2B_9H_{11})_2$ and single $NiC_2B_9H_{11}$ icosahedra require 102 and 60 electrons (PEC), respectively. In the latter, six nonbonding pairs are located at the Ni atom. According to Mingos' condensation rule, the PEC of the complete unit is equal to the sum of the individual counts for the parent polyhedra minus the count of the shared unit, or $2 \times 60 - 18 = 102$. When the shared atom is a main group element, as in the analogue $Si(C_2B_9H_{11})_2$, Mingos' condensation rule is taken as $A + B - 4$.[5] Each single unit of $SiC_2B_9H_{11}$ has a PEC of 50, which leads to a PEC of 96 for $Si(C_2B_9H_{11})_2$.

It appears that the count of a polyhedron condensed by vertex sharing depends on the nature of the polyhedron, but also on the size of the shared atom, as was reported by Burdett and Canadell.[11] They showed that only 12 SEPs are required for stabilization of the condensed $B(B_5H_5)_2$ unit instead of the 14 SEPs required by its analogue $Ga(B_5H_5)_2$. The reason invoked for this difference is that direct interactions between the two *nido* fragments are small when the shared atom is larger than atoms on the *nido* fragments. When the shared atom is of the same size, *nido*−*nido* interactions become strong enough to push some molecular orbitals into the antibonding domain. More recently, Vajenine and Hoffmann[28] have studied similar effects in chains and two-dimensional or three-dimensional networks formed by vertex-sharing aluminum octahedra.

In the gallium intermetallic compounds Li_5Ga_9 and $Na_{6.25}Rb_{0.6}Ga_{20.02}$,[12] vertex-sharing icosahedra exist, but the shared atom is a lithium or rubidium cation (in the latter compound, Rb is partially replaced by Ga). Electron counting in both structures shows the dimers to be stabilized with 52 skeletal electrons.

A molecular energy diagram has been calculated for a model composed of two *nido* gallium icosahedra in the *sss* configuration, conveniently saturated with hydrogen ligands (Figure 10). The positions of energy levels near to the gap have been represented in Figure 11 (left) as a function of *d*, the distance that separates the two pentagonal open faces. For a regular gallium icosahedron with all Ga−Ga distances equal to 2.60 Å, *y*, the height of the icosahedron pentagonal antiprism, is equal to 2.22 Å.

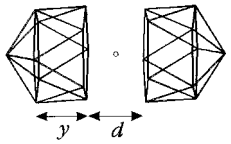

Figure 10. Two-*nido* icosahedron (*sss*) model used for the vertex-sharing analysis; *d* represents the separation parameter taken as a function of *y* (the height of the icosahedron pentagonal antiprism).

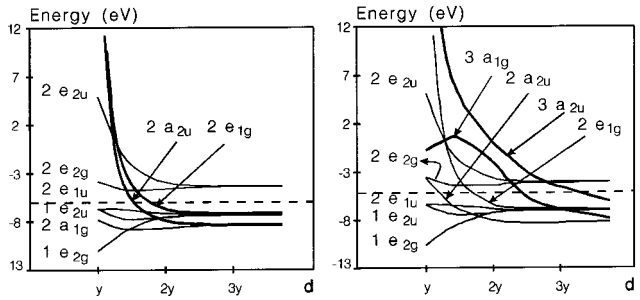

Figure 11. Walsh diagrams of two interacting *nido* icosahedral fragments separated by a distance *d*. Left: The fragments interact directly without an interstitial atom. Right: The fragments interact with an interstitial atom. Atoms have been considered with only two atomic orbitals, s and p_z (*z* along the 5-fold axis).

Scheme 4

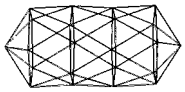

Scheme 5

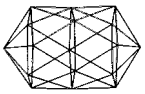

For a large separation of the two *nido* fragments ($d > 2y$), the polyhedral electron count is the sum of the two individual *nido* icosahedra counts, that is, 96 electrons. Reducing the interpolyhedral distance (*d* close to *y*) leads to a contracted di-icosahedron (Scheme 4). The electron count is reduced by six because the $2a_{2u}$ and $2e_{1g}$ levels are pushed upward in energy toward the antibonding region, so the PEC is then 90.

The *ses* configuration, with D_{5h} symmetry, is only possible when *d* is large enough to cancel the interactions between the two *nido* fragments; otherwise, the stable configuration would be the collapsed di-icosahedron (Scheme 5) for which a PEC of 70 is required. This polyhedron can be considered as resulting from the fusion of two *nido* icosahedra by the sharing of a pentagonal face. Its calculated electron count is the same as that obtained from Mingos' condensation rule. Each *nido* parent icosahedron has a PEC of 48, and the shared unit is a pentagon whose PEC would be that of $C_5H_5^-$ (26 electrons), so the PEC of the collapsed di-icosahedron is $2 \times 48 - 26 = 70$.

A vertex-sharing icosahedral dimer can be likened to two *nido* icosahedral fragments sandwiching an atom; this double unit displays D_{5d} symmetry (*sss* configuration). Electron counts have been determined as a function of the distance *d* separating the two open-pentagonal-face *nido* fragments (with the shared atom sitting halfway between the two fragments). Calculations have been performed for a gallium-containing model, for which the Walsh diagram is represented in Figure 11 (right). When *d* is large enough to cancel interactions between *nido* fragments ($d > 3y$), the system may be considered as two individual *nido*

(25) Kester, J. G.; Keller, D.; Huffman, J. A.; Benefiel, M. A.; Geiger, W. E.; Atwood, C., Jr.; Siedle, A. R.; Korba, G. A.; Todd, L. J. *Inorg. Chem.* **1994**, *33*, 5438.
(26) St. Clair, D.; Zalkin, A.; Templeton, D. H. *J. Am. Chem. Soc.* **1970**, *92*, 1173.
(27) This notation is used to describe the relative arrangement of the four pentagons in a vertex-sharing icosahedral dimer.
(28) Vajenine, G. V.; Hoffmann, R. *J. Am. Chem. Soc.* **1998**, *120* (17), 4200.

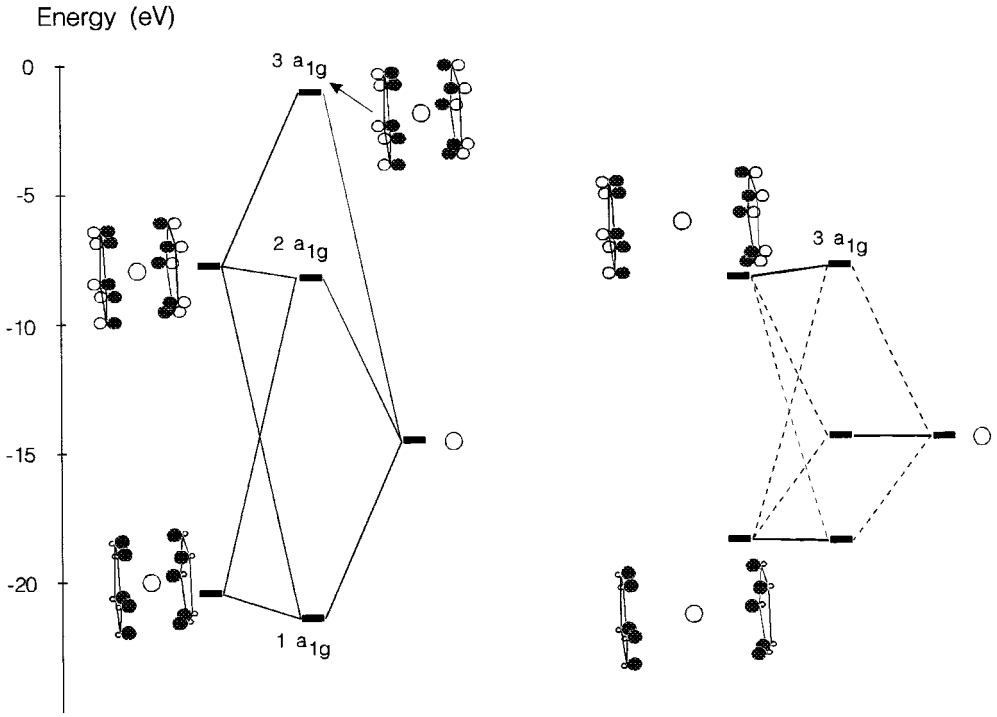

Figure 12. Schematic molecular orbital interaction diagram of vertex-sharing icosahedra restricted to the a_{1g} subset. Right: For d close to $3y$, the a_{1g} levels almost remain free from mixing. Left: For d close to y, the s orbital of the interstitial atom interacts with the sp orbitals of the pentagonal faces. Weak contributions from other atoms on the icosahedra have been neglected in the drawing.

icosahedra apart from an isolated atom. Bringing the icosahedra nearer to each other allows an interaction between AOs of the shared atom and frontier MOs of the fragment. The latter are mainly exo radial sp orbital combinations at the open pentagonal faces.

Among the resulting levels, the $3a_{1g}$ orbital exhibits an unusual behavior. It is bonding in nature for large values of d and becomes antibonding as d decreases, but this antibonding character is weakened for $d < 1.5y$. This behavior can be described in detail with an analysis of the a_{1g} molecular orbital subset. This subset can be analyzed with a three-level interaction in which the central atom participates only with its s orbital, while the atoms on the pentagonal open faces participate with sp orbitals. One fragment's molecular level has a strong s character, while the other's is primarily p (see Figure 12). For large values of d, there is no important mixing of these levels with the s orbital of the interstitial atom, and the $3a_{1g}$ level is π-bonding within the pentagons. When d decreases, an antibonding interaction with the s orbital of the interstitial atom pushes the $3a_{1g}$ orbital up toward high energies. This destabilizing effect is compensated as soon as the pentagonal faces come closer to each other (d on the order of $1.5y$), because additional direct bonding overlap of the pentagon MOs is allowed and the $3a_{1g}$ level moves toward lower energies.

The $3a_{2u}$ level results from the interaction of the pentagon MOs with the p_z orbital of the shared atom. A decrease in d successively induces the expulsion from the bonding domain of the $3a_{2u}$ and $3a_{1g}$ levels, reducing the polyhedral electron count by two and then by four (Figure 11).

As mentioned above, the carborane $Si(C_2B_9H_{11})_2$ molecule has a polyhedral count of 96 electrons; subtracting 44 electrons for B−H exo bonds leads to a skeletal electron count of $52 = 2 \times 26 - 0$. Not surprisingly, $Ni(C_2B_9H_{11})_2$, in which $d = 2y$, has the same skeletal electron count, as could be expected because Si and Ni have similar covalent radii (1.173 and 1.154 Å, respectively).

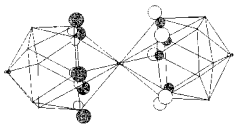

Figure 13. Representation of the $2a_{2u}$ molecular orbital. This orbital, the HOMO when d is on the order of $1.5y$, is pushed up toward the antibonding domain when d decreases.

A further decrease of d raises the $2e_{1g}$ level up toward higher energy (Figure 11). The $2a_{2u}$ level (Figure 13), which is the HOMO when d is on the order of $1.5y$, is π-bonding within the open pentagonal faces (Figure 13). The interaction of *nido* fragment orbitals with orbitals of the shared atom, mainly the p_z orbitals, is also bonding. Antibonding overlap between the *nido* fragments increases as d becomes smaller. For $d \ll 1.5y$, the $2a_{2u}$ level is pushed up into the antibonding region, bringing the polyhedral electron count to 94.

Edge-Sharing Icosahedra. Clusters can also condense by sharing edges. Some examples are known for small polyhedra that share opposite edges to form infinite chains, as do tetrahedra in $KFeS_2$[29] or octahedra in the transition element halides NbX_4 and TaX_4.[30] Among Zintl phases of group 13 elements, $NaGa_4$ ($BaAl_4$ structural type) is formed by square pyramids (distorted *nido* octahedra) sharing edges to form a bidimensional anionic network.[31] Mingos' condensation rule predicts that the polyhedral electron count is $A + B - 14$ for the edge-sharing polyhedra ($A + B - 34$ if the shared edge is composed of d elements).

To our knowledge, edge-sharing, nondefective icosahedra have not been found, as such a regular unit would be unstable with regard to interactions between atoms having interatomic distances l that are too short (Scheme 6). In the case of a regular gallium icosahedra with all Ga−Ga bonds equal to 2.6 Å, $l = 1.6$ Å. Elongation of l would progressively transform the system

(29) Whangbo, M. H.; Foshee, M. J. *Inorg. Chem.* **1981**, *20*, 113.
(30) Silvestre, J.; Hoffmann, R. *Inorg. Chem.* **1985**, *24*, 4108.
(31) Bruzzone, G. *Acta Crystallogr.* **1969**, *B25*, 1206.

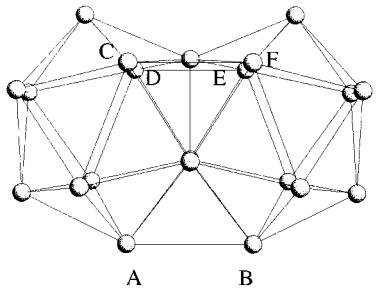

Compound	Ref.	Site occupations (%)					
		A	B	C	D	E	F
$Li_9K_3Ga_{28.83}$	[*34*]	51	0	100	100	16	16
$Li_3Na_5Ga_{19.57}$	[*35*]	60	60	53	53	53	53
$Na_{6.25}Rb_{0.6}Ga_{20.02}$	[*36*]	51	51	81	81	81	81
α- AlB_{12}	[*37*]	100	100	0	100	0	100
γ- AlB_{12}	[*38*]	100	100	0	0	100	100
α-tetragonal B	[*39*]	100	100	100	100	100	100

Figure 14. Representation of the twinned icosahedron. Sites labeled A−F are prone to atomic defects. Site occupations in selected compounds are reported.

Scheme 6

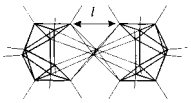

Scheme 7

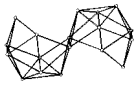

into two *arachno* icosahedra sandwiching a dumbbell (Scheme 6), and some electron relocalization would occur at the dumbbell.

To suppress antibonding interactions between icosahedral units, better stabilization of edge-sharing icosahedra is afforded by the ejection of at least two atoms. This is observed in *n*-$B_{18}H_{22}$ borane (Scheme 7), which results from condensation by edge sharing of two $B_{10}H_{14}$ *arachno* icosahedra.[32] A polyhedral electron count of 76 is required for this molecule to attain a closed shell configuration.

Face-Sharing Icosahedra. Oligomeric units can also form by the face-sharing condensation (otherwise called fusion) of icosahedra. The dimer is referred to as a twinned icosahedron. The trimer and the tetramer, in which each basic icosahedral unit shares a triangular face with each of its neighbors, will be called the triply fused icosahedron and the tetra-fused icosahedron, or merely the tri-icosahedron and the tetra-icosahedron, respectively.

Twinned Icosahedra. Twinned icosahedra are commonly found in intermetallic phases of gallium and boron. A nondefective twinned icosahedron (Figure 14) is present in α-tetragonal boron.[39] All atoms within the twinned icosahedron, except for those on the shared triangle, are outwardly bonded. EHMO calculations show that 82 electrons are required for stabilization of the twinned icosahedron. Subtracting the 36 electrons involved in the 18 exo bonds leads to a skeletal electron count of 46 ($2 \times 26 - 6$), in agreement with Mingos' rules. In recent MO calculations,[33] the twinned icosahedron has been analyzed using different models: two interacting *closo* and *hypho* icosahedra or two *hypho* icosahedra sandwiching a triangle. The results indicate strong interactions between atoms C and F and D and E (see Figure 14).

Table 1. Calculated Overlap Populations for Bonds within $Ga_{21}H_{14}$ (Bold) and $Ga_{21}H_{18}$ (Italic) Clusters

	74 e$^-$	76 e$^-$	78 e$^-$	80 e$^-$	82 e$^-$	84 e$^-$
A−B	**0.23**	**0.21**	**0.22**	**0.21**		
		0.19	*0.20*	*0.18*	*0.16*	*0.44*
C−F	**0.53**	**0.50**	**0.61**	**0.49**		
		0.20	*0.22*	*0.19*	*0.17*	*0.43*
all bonds	**0.40**	**0.41**	**0.42**	**0.41**		
		0.36	*0.37*	*0.38*	*0.39*	*0.38*

The twinned icosahedron is often found to be atom-defective (Figure 14). In gallium intermetallic compounds, when atoms A and B are present, they are exo bonded to neighboring clusters, whereas atoms C, D, E, and F are not. Except for atoms at the shared triangle, all remaining atoms are exo-bonded. This fact led us to the model $Ga_{21}H_{14}$, in which hydrogen ligands are used to simulate exo bonds. In $Ga_{21}H_{18}$, equivalent to the $B_{21}H_{18}$ model,[33] hydrogen ligands have also been attached to atoms C, D, E, and F.

For $Ga_{21}H_{18}$ (Figure 14), a consistent energy gap is found for 82 electrons, and overlap populations indicate that the addition of extra electrons would destabilize the system. Interestingly, overlap populations for the C−F (D−E) and A−B bonds, with values of 2.61 and 2.83 Å, respectively, are relatively low (0.17 and 0.16 at the HOMO, respectively) and decrease continuously from 78 to 84 electrons. Although globally bonding, the two highest-occupied orbitals (at approximately −8 eV) have antibonding character at the C−F (D−E) and A−B edges, whereas at the LUMO (−6 eV, globally antibonding), contributions from these edges are bonding.

As indicated in Table 1, the $Ga_{21}H_{14}$ cluster reaches a maximum bonding overlap for 78 electrons. This count also corresponds to a maximum in the calculated overlap populations for the C−F (D−E) and A−B bonds. A look at Figure 15 (right) shows that, in this case, the HOMO, the LUMO, and the orbital just above have mainly C, D, E, and F atomic orbital contributions. The C−F (D−E) edges are π-bonding at the HOMO level and π-antibonding at and above the LUMO level.

Inasmuch as 28 electrons are involved in exo bonding with hydrogen atoms, there remain $78 - 28 = 50$ electrons for Ga−Ga skeletal bonding. If 2c-2e bonds are assumed for the C−F (D−E) edges (2.61 Å), the skeletal electron count is 46. Removal of one atom among the sites A−F does not modify the skeletal electron count of the cluster, nor does removal of any combination of these atoms (Figure 16).

Molecular orbitals near −6 eV are antibonding at the C−F and D−E edges. Removal of the corresponding atoms increases the energy gap (Figure 16, right). Although the full $Ga_{21}H_{14}$ or the atom-defective derivatives are stable, there is a marked stabilization of defective polyhedra in which antibonding

(32) Simpson, P. G.; Folting, K.; Dobrott, R. D.; Lipscomb, W. N. *J. Chem. Phys.* **1963**, *39*, 2339.
(33) Burdett, J. K.; Canadell, E. *Inorg. Chem.* **1991**, *30*, 1991.
(34) Belin, C. *J. Solid State Chem.* **1983**, *50*, 225.
(35) Charbonnel, M.; Belin, C. *Nouv. J. Chim.* **1984**, *10*, 595.
(36) Charbonnel, M.; Belin, C. *J. Solid State Chem.* **1987**, *67* (2), 210.
(37) Vlasse, M.; Boiret, M.; Naslain, R.; Kasper, J. S.; Ploog, J. *C. R. Acad. Sci. Paris* **1978**, *C287*, 27.
(38) Vlasse, M.; Naslain, R.; Kasper, J. S.; Ploog, K. *J. Solid State Chem.* **1979**, *28*, 289.
(39) Hughes, R. E.; Leonowicz, M. E.; Lemley, J. T.; Tai, L. T. *J. Am. Chem. Soc.* **1977**, *99* (16), 5507.

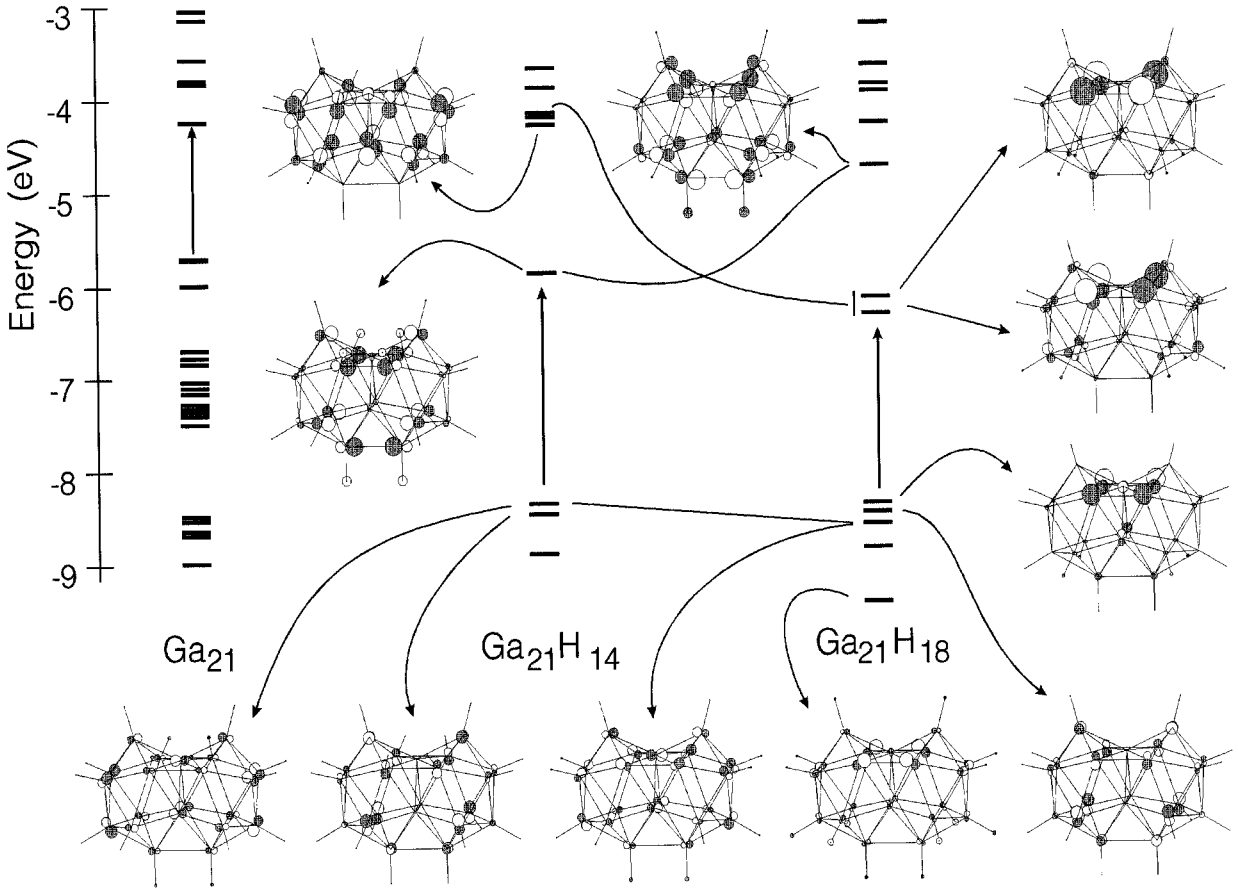

Figure 15. Energy diagrams for the naked Ga_{21} (left) and the $Ga_{21}H_{18}$ (middle) and $Ga_{21}H_{14}$ (right) clusters. Some molecular orbitals of particular interest have been represented.

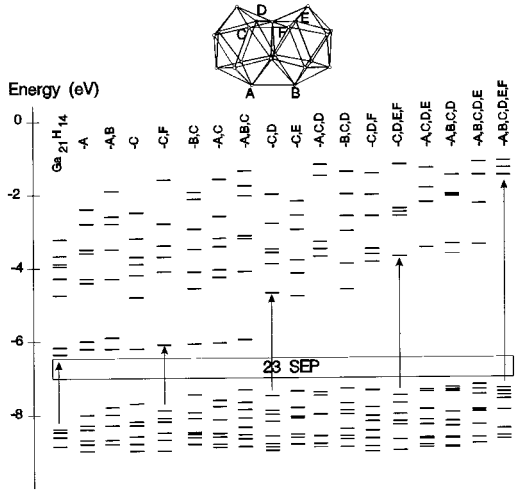

Figure 16. MO energy diagrams for the twinned icosahedron $Ga_{21}H_{14}$ and atom-defective derivatives. The skeletal electron count (23 SEP) remains unchanged in all cases.

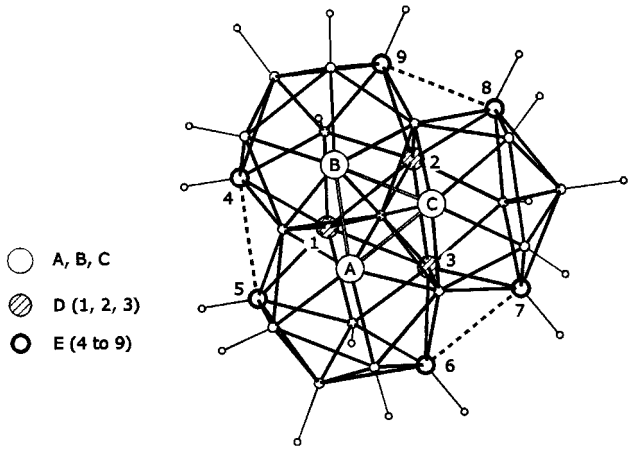

Figure 17. Triply fused icosahedron or tri-icosahedron. Atomic defects occur at the particular sites labeled A−E.

interactions between neighboring atoms are suppressed. In solid-state chemistry, stabilization of these twinned icosahedra may also depend on packing limitations, polarization, and size tuning with alkali cations.

Triply Fused Icosahedra. The rhombohedral structures of $Na_{13}K_4Ga_{47.45}$[40] and $Na_{21}K_{14}Cd_{17}Ga_{82}$,[41] in addition to the icosahedron, contain the triply fused icosahedron (tri-icosahedron). Such a polyhedron is also a building unit in β-rhombohedral boron structure.[42−44]

The M_{28} tri-icosahedron (Figure 17) results from the condensation of three icosahedra, in which each icosahedron shares a triangular face with each of its neighbors and one atom (on the 3-fold axis) is common to the three icosahedra. Tri-icosahedra, like twinned icosahedra, are generally found with atomic

(40) Flot, D.; Vincent, L.; Tillard-Charbonnel, M.; Belin, C. *Acta Crystallogr.* **1998**, *C54*, 174.
(41) Flot, D.; Vincent, L.; Tillard-Charbonnel, M.; Belin, C. *Z. Kristallogr.* **1997**, *212*, 509.
(42) Hoard, J. L.; Sullenger, B.; Kennard, C. H.; Hugues, R. E. *J. Solid State Chem.* **1970**, *1*, 268.
(43) von Geist, D.; Kloss, R.; Follner, H. *Acta Crystallogr.* **1970**, *B26*, 1800.
(44) Callmer, B. *Acta Crystallogr.* **1977**, *B33*, 1951.

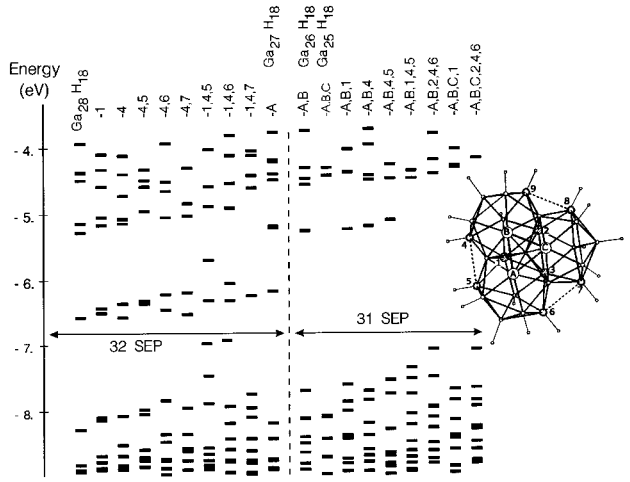

Figure 18. MO energy diagrams for the $Ga_{28}H_{18}$ tri-icosahedron and atom-defective derivatives. For clarity, atoms at position D are labeled 1−3 and atoms at position E, 4−9.

defects on particular sites. In $Na_{13}K_4Ga_{47.45}$, the tri-icosahedron is connected through a maximum of 18 exo bonds to neighboring clusters; thus, EHMO calculations have been carried out for the $Ga_{28}H_{18}$ molecular unit and also for its defective derivatives.

A nondefective tri-icosahedron requires a polyhedral count of 100 electrons (closed shell), of which 64 are for skeletal stabilization and 36 for exo bonding. The appropriate PEC of 100 would be matched for the $Ga_{28}H_{18}^{2+}$ cation, the existence of which is quite unlikely in a Zintl-phase (reducing) environment. We have shown that in the nondefective $Ga_{28}H_{18}$ polyhedron (C_{3v}), exo sp-type orbitals at atoms A, B, and C overlap into one bonding (a_1, −9 eV) and two antibonding (e, LUMO) π-type combinations (see Figure 21 for orbital representations). The two extra electrons for the $Ga_{28}H_{18}$ neutral molecule would populate the degenerate LUMO, yielding an unstable electronic configuration prone to Jahn−Teller distortion. As will be discussed below, a more stable configuration is obtained when atoms (one, or better, two) are expelled from the ABC triangle.

We will now examine the effects that atomic defects observed in $Na_{13}K_4Ga_{47.45}$[40] have on the tri-icosahedron electron count. There are three sets of defect sites: A (B, C), D, and E (Figure 17). In accord with their crystallographically refined site occupations, 0.18, 0.77, and 0.77, respectively, different H-saturated molecular models have been considered. Molecular orbital energy diagrams relative to various combinations of A (B, C), D, and E atomic defects are depicted in Figure 18. A skeletal electron count of 64 (32 SEP) is retained to reach a closed shell in all configurations in which only D and E defects occur (Figure 18, left).

The tri-icosahedron occurs in $Na_{13}K_4Ga_{47.45}$ (see Figure 19) as pairs inverted through a $\bar{3}m$ center, and it is connected to surrounding polyhedra through 2c-2e bonds. Of the six equivalent positions A, B, and C, and the inverted A′, B′, and C′, only one is occupied (the crystal site occupation was refined to 0.18). Thus, we may consider the inverted pair as formed of a doubly *nido* and a triply *nido* tri-icosahedron (Figure 20). As for the nondefective M_{28} tri-icosahedron, each of these clusters (M_{26} and M_{25}) has 18 exo bonds. Bonding within these polyhedra, particularly at the ABC triangle, was analyzed by EHMO calculations. For this purpose, energy diagrams were calculated for the $Ga_{28}H_{18}$ polyhedron and its three *nido* (missing one or more of the atoms A, B, and C) derivatives $Ga_{27}H_{18}$, $Ga_{26}H_{18}$, and $Ga_{25}H_{18}$ (Figure 18). The energy gap (1.7 eV for

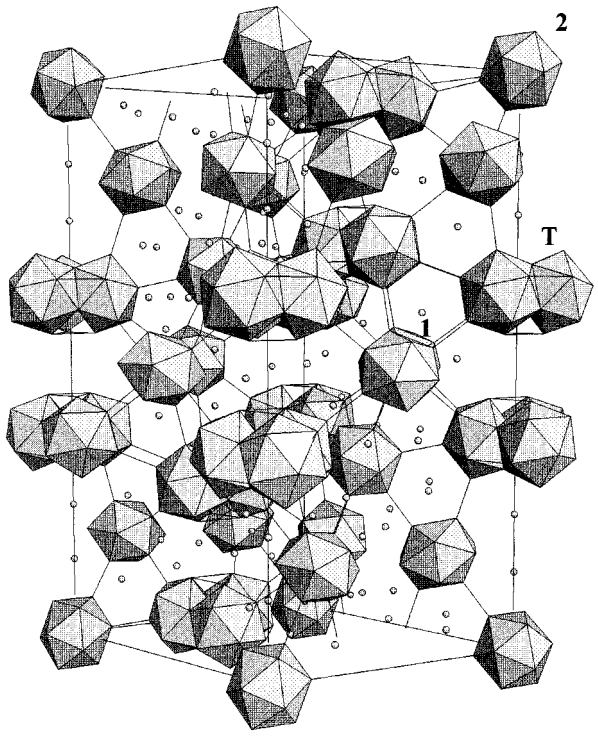

Figure 19. Representation of the crystal structure of $Na_{13}K_4Ga_{47.45}$, in which tri-icoshaedra (T) appear as inverted pairs (atomic defects are not represented). The labels 1 and 2 indicate the two kinds of icosahedra.

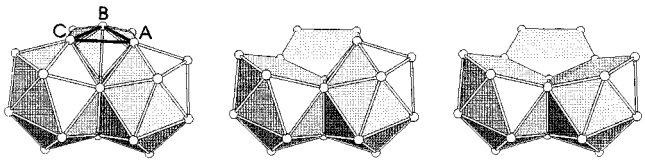

Figure 20. Triply fused icosahedron or tri-icosahedron and its *nido* derivatives. Nondefective (left), doubly *nido* (middle), and triply *nido* (right) polyhedra.

$Ga_{28}H_{18}$) increases with the number of missing A, B, and C atoms (2.0, 2.4, and 3.7 eV for one, two, and three missing atoms, respectively). MOOPs (molecular orbital overlap populations) are represented in Figure 21; they allow a better understanding of bonding within the polyhedron. As R. Hoffmann explained,[45] MOOPs represent a "*solid-state way* to plot crystal orbital overlap populations curves (overlap population-weighted density of states) for a molecule".

For the nondefective $Ga_{28}H_{18}$ polyhedron (C_{3v}), overlap populations indicate that interactions between the A, B, and C atoms are bonding up to 94 valence electrons. The upper occupied level (a_1) essentially results from the combination of sp (parallel to the 3-fold axis) orbitals at the A, B, and C atoms and at the tetrahedral core of the cluster (Figure 21). Filling levels up to the gap (100 electrons, 32 SEP) does not globally destabilize the polyhedron because the A, B, and C atoms make no contribution to these levels. The degenerate LUMO primarily involves the A, B, and C atoms and displays a lone-pair character with some repulsion effects, as indicated by the slight antibonding character of this molecular orbital. This effect is crucial when two inverted units are considered together.

In the one-*nido* $Ga_{27}H_{18}$ tri-icosahedron (C_s), one atom is missing at the upper triangle, the HOMO (a′) has no contribution

(45) Hoffmann, R. *Rev. Mod. Phys.* **1988**, *60* (3), 601.

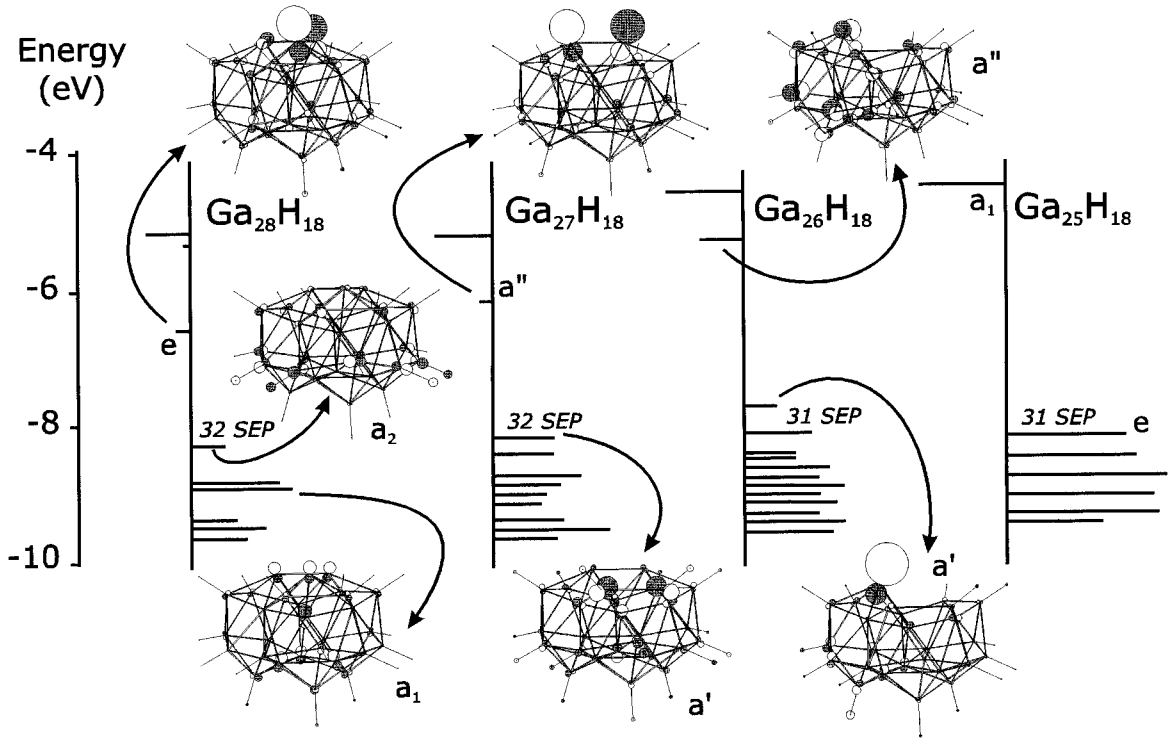

Figure 21. Molecular orbital overlap populations (MOOP, the molecular analogue of COOP) for the nondefective $Ga_{28}H_{18}$ tri-icosahedron and for its *nido* derivatives $Ga_{27}H_{18}$, $Ga_{26}H_{18}$, and $Ga_{25}H_{18}$.

from remaining A and B atoms, and the LUMO (a″) still displays a repulsive, lone-pair character. When two atoms are removed from the ABC triangle ($Ga_{26}H_{18}$, doubly *nido* tri-icosahedron, C_s), the lone-pair orbital at the remaining atom is found at the HOMO (a′). Interactions are bonding up to the addition of 100 electrons, but because of the strong lone-pair character of the HOMO, the $Ga_{26}H_{18}$ cluster could be considered to be stabilized with 62 skeletal electrons (31 SEP). The $Ga_{25}H_{18}$ triply *nido* tri-icosahedron (C_{3v}) has a degenerate HOMO and still maintains a skeletal electron count of 62 (31 SEP).

Tri-icosahedra are also found as inverted pairs in $Na_{14}K_{21}Cd_{17}Ga_{82}$[41] with Cd atomic defects at the ABC triangles. Also in this phase, over the six A, B, and C, and A′, B′, and C′ sites, only one is statistically occupied. All of the other atomic positions are completely filled, but some of them show a Cd/Ga occupational disorder. Atomic substitution provides some relaxation to the cluster (enlargement of the upper triangle), and a closed shell is also attained with 62 skeletal electrons.

Tetra-Icosahedra. The tetra-icosahedron results from the fusion of four tetrahedrally arranged icosahedra. Each icosahedron shares a triangular face with each of its three neighbors, and the shared faces form the core tetrahedron. So far, this 34-atom cluster has not been found in intermetallic phases of group 13 elements and alkali metals, but it exists as a building block in tcp-related structures of the γ-brass type (tcp denotes tetrahedrally close-packed). The skeletal electron count of 82 is appropriate for the stabilization of the isolated 34-atom unit, conveniently saturated with hydrogen ligands. The formation of the tetra-icosahedron is favored by the incorporation of smaller atoms at the centers of the icosahedra and at the core tetrahedron, as observed in Fe−Zn alloys.[46]

Extended Structures Containing Condensed Icosahedra. Among ternary and quaternary intermetallic phases of gallium and alkali metals, the orthorhombic phases $Li_9K_3Ga_{28.83}$,[34] $Li_3Na_5Ga_{19.57}$,[35] $Rb_{0.6}Na_{6.25}Ga_{20.02}$,[36] and $Na_{128}Au_{81}Ga_{275}$[47] contain twinned icosahedra, whereas the rhombohedral phases $Na_{13}K_4Ga_{47.45}$[40] and $Na_{14}K_{21}Cd_{17}Ga_{82}$[41] contain tri-icosahedra occurring as atom-defective inverted units.

Table 2. Some Geometric Features of the Tri-Icosahedron Inverted Pairs in Intermetallic Phases of Gallium

	nature of atom		distance (Å)	
	ABC	N[a]	A−B	*h*[b]
$Na_{13}K_4Ga_{47.45}$	Ga	−	2.52	3.49
$Na_{14}K_{21}Cd_{17}Ga_{82}$	Cd	−	2.70	3.76
$Na_{17}Cu_6Ga_{46.5}$	Cu/Ga	Cu	2.76	3.96
$Na_{17}Zn_{12}Ga_{40.5}$	Zn/Ga	Zn	2.83	3.82
$Na_{34}Cu_7Cd_6Ga_{92}$	Cu	Cu	2.77	3.94

[a] N represents the interstitial atom type. [b] *h* represents the separation between the inverted ABC and A′B′C′ triangles.

The stability of the nondefective tri-icosahedron inverted pair ($2 \times M_{28}$) is increased when some of the gallium atoms are replaced by smaller and more electron-poor atoms (such as Cu and Zn). This relaxes the polyhedral framework, enlarges the ABC and A′B′C′ triangles, and increases the separation of the triangles (Table 2). Insertion of an interstitial atom N at the center $\bar{3}m$ to form the complex polyhedron $(M_{28})_2N$ (Figure 22) also has a stabilizing effect. Such units have been found in the compounds $Na_{17}Cu_6Ga_{46.5}$,[48] $Na_{17}Zn_{12}Ga_{40.5}$,[49] and $Na_{34}Cu_7Cd_6Ga_{92}$.[50] In the latter, the polyhedron $(Ga_{25}Cu_3)_2Cu$ contains a $(Cu_3)_2Cu$ trigonal antiprismatic core.

EHMO calculations for the molecular $(Ga_{28})_2N$ unit with N = Cu or Zn, conveniently saturated with hydrogen ligands,

(46) Belin, C.; Belin, R. *J. Solid State Chem.* **2000**, *150*, in press.
(47) Tillard-Charbonnel, M.; Belin, C.; Chouaibi, A. *Z. Kristallogr.* **1993**, *206*, 310.
(48) Tillard-Charbonnel, M.; Chouaibi, N.; Belin, C.; Lapasset, J. *J. Solid State Chem.* **1992**, *100* (2), 220.
(49) Tillard-Charbonnel, M.; Chouaibi, N.; Belin, C. *C. R. Acad. Sci. Paris* **1992**, *315*, 661.
(50) Chahine, A.; Tillard-Charbonnel, M.; Belin, C. *Z. Kristallogr.* **1994**, *209*, 542.

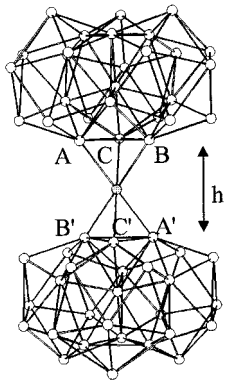

Figure 22. Complex polyhedron $(M_{28})_2N$ that results from the incorporation of an interstitial atom at center $\bar{3}m$ of the tri-icosahedron inverted pair.

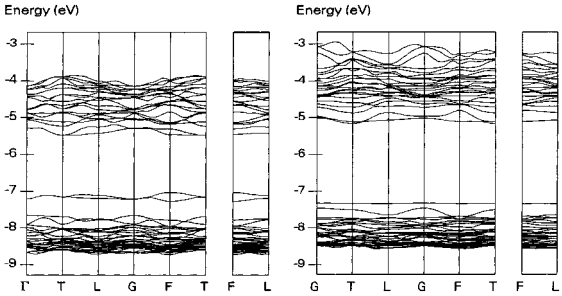

Figure 23. Band structure for $Na_{13}K_4Ga_{49.57}$ containing defective tri-icosahedra (right) and for the hypothetical $Na_{13}K_4Ga_{52}$ containing nondefective tri-icosahedra (left).

indicate that 204 electrons are required for a closed shell, of which 132 are skeletal electrons (66 SEP). Saturated d orbitals of the heteroatom Cu or Zn do not contribute to the bonding. Orbital interactions of the interstitial atom at the center of an antiprism have been depicted in Figure 7. The six fragment orbitals (exo in character) interact with the s and p atomic orbitals of the interstitial atom to provide four bonding MOs (a_{1g}, a_{2u}, and e_u in D_{3d} symmetry). Eight electrons are to be added to the sum of skeletal electron counts for two M_{28} units, so that $(M_{28})_2N$ is stabilized with $2 \times 62 + 8 = 132$ skeletal electrons.

This molecular approach was completed by the band analysis of the three-dimensional periodic framework of $Na_{13}K_4Ga_{47.45}$ (Figure 19) whose structure is built with two kinds of icosahedra (1 and 2) having different symmetries and with tri-icosahedra. Because of the nonstoichiometric character of the ABC triangle of the tri-icosahedron, the rhombohedral cell of $Na_{13}K_4Ga_{47.45}$ has been considered as two tri-icosahedra, one doubly *nido* and the other triply *nido*. In this phase, there is no interstitial atom N between the inverted tri-icosahedra. Additional atomic defects (25% at crystallographic sites 18h and 36i) within the trimeric icosahedral unit have been neglected in building a periodic model having $Na_{13}K_4Ga_{49.57}$ stoichiometry. The band structure has been calculated for 34 k-points taken on special symmetry paths and densities of states with a grid of 32 k-points in the IBZ. Calculations have also been performed for a $Na_{13}K_4Ga_{52}$ framework in which there would be no atomic defects (two nondefective tri-icosahedra).

The band structure for $Na_{13}K_4Ga_{49.57}$ (one doubly *nido* and one triply *nido* tri-icosahedron) displays two groups of bands separated by a gap of nearly 2 eV (Figure 23, right). The valence band would be entirely filled with 314 electrons (two formula units in the rhombohedral cell). The highest-occupied crystal orbital has no dispersion and displays a lone-pair character at

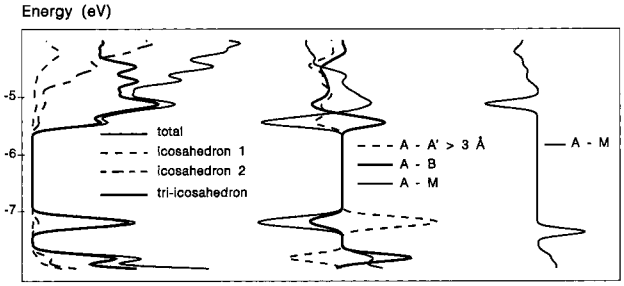

Figure 24. Projected densities of states for individualized and for triply fused icosahedra in the hypothetical $Na_{13}K_4Ga_{52}$ (left). COOP curves for bonds involving atom A (B, C) for $Na_{13}K_4Ga_{52}$ (middle) and for the periodic model $Na_{13}K_4Ga_{49.57}$ (right). Within the tri-icosahedron, A, A′, and B refer to the atoms on the triangle and M refers to the remaining atoms. Respective contributions of the two kinds of icosahedra (different symmetries) are represented.

atom A (crystal orbital analysis at Γ). Partial DOS for the tri-icosahedron is in agreement with the skeletal electron count of 62 that was previously determined.

For $Na_{13}K_4Ga_{52}$ (nondefective polyhedra), dispersion curves also display two groups of bands separated by nearly 2 eV (Figure 23, left). The valence band would be entirely filled with 320 electrons. Crystal orbitals on each side of the gap, at −7.2 and −5.3 eV, are of interest; they are degenerate at the BZ center (Γ) and originate primarily from the tri-icosahedron molecular orbitals. Weak dispersion for crystal orbitals at −7.2 eV (top of the valence band) indicates a globally nonbonding character. COOP curves (Figure 24) show that antibonding interactions within the tri-icosahedron (bonds of 2.52 Å at the ABC triangle and A−M bonds from 2.56 to 2.67 Å between the triangle and the remainder of the tri-icosahedron) are globally balanced by bonding interactions between triangles of inverted unit (A−A′ bonds). Despite some bonding character at the ABC triangle, the crystal orbital lying at −5.3 eV is globally antibonding. For the hypothetical $Na_{13}K_4Ga_{52}$, with 346 valence electrons, the antibonding band would be populated up to −4.3 eV.

It is evident that, to reach a stable configuration, the "structure" requires a reduced valence electron count; this condition is appropriately fulfilled by the expulsion of atoms from the ABC (A′B′C′) triangles of the tri-icosahedra. For the $Na_{13}K_4Ga_{49.57}$ periodic model, the valence electron count would be 331 (two formula units), exceeding the ideal (closed-shell) count of 314 by 17 electrons. The actual valence electron count of 319 for the experimental $Na_{13}K_4Ga_{47.45}$ compound, in which some supplementary atomic defects occur, is quite satisfactory within the uncertainty limits of the structural determination.

The compound $Na_{14}K_{21}Cd_{17}Ga_{82}$ displays the same polyhedral packing, in which the replacement of some gallium atoms by more electron-poor cadmium atoms reduces the valence electron count to 315.

Substitution of gallium atoms by heteroelements also occurs in the rhombohedral phases $Na_{17}Cu_6Ga_{46.5}$, $Na_{17}Zn_{12}Ga_{40.5}$, and $Na_{34}Cu_7Cd_6Ga_{92}$, which contain interstitial atoms at the $\bar{3}m$ center of tri-icosahedron pairs. Their valence electron counts are 325, 325, and 330, respectively. The band structure has been calculated for $Na_{34}Cu_7Cd_6Ga_{92}$ (primitive rhombohedral cell, $Z = 1$). COOP curves show that filling bands to −7.4 eV would require 320 electrons, with a total overlap population of 0.4246. The HOMO, degenerate at Γ, results essentially from the copper core $(Cu_3)_2Cu$. Filling levels above 320 electrons is not very destabilizing, as it only decreases the overlap population to 0.4244 (324 electrons), 0.4236 (328 electrons), and 0.4222 (330 electrons).

Concluding Remarks

Numerous experimental and theoretical studies have been published in the field of cluster chemistry. Icosahedron-based clustering is very common in the intermetallic chemistry of transition metals and early p-block elements. Counting electrons in clusters has proved to be a very useful and elegant method for rationalizing geometries and interpreting the frameworks of which clusters are the building blocks. On the basis of some valence bond ideas, it is possible to find correlations between bonding in the structure, valence electron concentrations, and electronic requirements.

Among the electron counting methods, the Wade-Mingos PSEPT approach is the most widely used for the interpretation of deltahedral clusters of main group elements. Unfortunately, these rules fail for large deltahedral clusters (icosa-octahedra, etc.), for clusters whose geometries consistently deviate from sphericity, and for the majority of atom-defective clusters and complex condensed clusters.

Valence electron concentrations per atom correlate fairly well with the degree of polymerization observed in icosahedron-based extended structures. Isolated icosahedra are found in thallium intermetallic phases with alkali metals, such as, the Tl-centered icosahedron in $Na_4A_6Tl_{13}$ (A = K, Rb, or Cs),[23] in which the mean electron concentration per Tl is 3.85. Interconnected icosahedral clusters are typical in intermetallic Zintl-type phases of group 13 elements. When each atom of the icosahedron is 2c-2e exo-bonded, the valence electron concentration per cluster atom drops substantially to 3.16. Various intermediate situations are found in the intermetallic compounds of gallium. In addition to 12 exo-bonded icosahedra, $Na_{22}Ga_{39}$[51] and Na_7Ga_{13}[52] contain incompletely exo-bonded icosahedra and (low-coordinate) 15-atom spacers. In this case, the valence electron concentration per gallium atom on the different icosahedral units varies from 3.16 to 3.67. Generally, in alkali metal-poor phases or in phases containing group 11 or 12 elements, electron concentrations are such that no low-coordinate (reduced) atoms are present. Condensation into fused clusters occurs as soon as the valence electron concentration comes close to 3.0. This is nicely illustrated for triply fused icosahedra in the rhombohedral structures of $Na_{13}K_4Ga_{47.45}$[40] and $Na_{17}Zn_{12}Ga_{40.5}$.[49] At lower electron concentrations, there is no longer any localized inter-polyhedral bonding, as icosahedra are condensed through smaller clusters such as in $NaZn_{13}$, in which the electron concentration is close to 2.1. The ultimate is reached with tcp structures such as Cu_5Zn_8, whose cluster electronic requirements match the Hume−Rothery valence electron concentration criterion (1.62 for γ-brass alloys).

Acknowledgment. We thank Martin Köckerling for having kindly provided us with a PC adaptation of the EHT band calculation program.

Appendix: Exponents and parameters used in calculations

atom	orbital	H_{ii} (eV)	$\xi(C_1)^a$	$\xi(C_2)^a$
H	1s	−13.60	1.33	
B	2s	−15.20	1.30	
	2p	−8.50	1.30	
C	2s	−21.40	1.625	
	2p	−11.40	1.625	
Al	3s	−12.65	1.55	
	3p	−8.00	1.55	
Si	3s	−17.30	1.383	
	3p	−9.20	1.383	
Ni	3d	−13.70	5.75 (0.5862)	2.20 (0.5846)
	4s	−10.95	2.1	
	4p	−6.27	2.1	
Cu	3d	−14.00	5.95 (0.5933)	2.30 (0.5742)
	4s	−11.40	2.2	
	4p	−6.06	2.2	
Zn	3d	−15.00	5.95 (0.5933)	2.30 (0.5744)
	4s	−12.41	2.01	
	4p	−6.53	1.70	
Ga	4s	−14.58	1.77	
	4p	−6.75	1.55	
Cd	4d	−14.60	6.38 (0.6404)	2.81 (0.5203)
	5s	−12.50	2.30	
	5p	−6.60	2.10	
Mo	4d	−10.50	4.54 (0.5899)	1.90 (0.5899)
	5s	−8.34	1.96	
	5p	−5.24	1.90	
Tl	6s	−16.20	2.37	
	6p	−9.00	1.97	

[a] Contraction coefficients used in the double-ξ expansion.

IC9910817

(51) Ling, R. G.; Belin, C. *Acta Crystallogr.* **1982**, *B38*, 1101.
(52) Frank-Cordier, U.; Frank-Cordier, G.; Schäfer, H. *Z. Naturforsch.* **1982**, *37b*, 119; **1982**, *37b*, 127.